Solid-State ^{13}C and ^{15}N NMR Analyses of Structure and Dynamics of Spacer Methylene Sequences and Mesogen Groups for Liquid Crystalline Polyurethanes with Different Spacer Lengths

Hiroyuki Ishida and Fumitaka Horii*

Institute for Chemical Research, Kyoto University, Uji, Kyoto 611-0011, Japan

Received February 25, 2002

ABSTRACT: Solid-state ^{13}C NMR analyses of the structure and dynamics have been performed for liquid crystalline polyurethanes with different spacer CH_2 lengths, which were polymerized from 3,3′-dimethyl-4,4′-biphenyldiyl diisocyanate, α,ω-alkanediols having various even numbers *m* of carbons, and 1-hexanol. Each sample was crystallized by cooling from the melt through the liquid crystalline phase at an appropriate cooling rate depending on its phase transition behavior detected by DSC. ^{13}C spin−lattice relaxation analyses have revealed that each CH_2 carbon resonance line contains three components with different T_{1C} values which are assigned to the crystalline, medium, and noncrystalline (supercooled liquid crystalline) components. For the polyurethane samples with $m = 8$ and 12, it has been found that the spacer CH_2 sequences for the noncrystalline component will adopt the alternate *trans* (*t*) and *trans*−*gauche* exchange (*x*) conformation in the central part whereas those of the crystalline and medium components may be in the *all-trans* conformation. Accordingly, the conformation of the spacer CH_2 sequences can be generally expressed as $ttx(tx)_{\ell}tt$ ($\ell = m/2 - 3$) for $8 \le m \le 12$, including the result for $m = 10$ reported previously. Furthermore, to examine molecular motion of the mesogen units in detail, ^{13}C CSA spectra have been measured at room temperature for the mesogen carbons by 2D SASS ^{13}C NMR spectroscopy and compared with those simulated by using the two-site exchange model for the flip motions of the phenylene group. As a result, it has been suggested that flip angles of fluctuations around the phenylene axis may be limited to less than about 20° without any 180° flip motion in all components, including the supercooled liquid crystalline component. Natural abundant CP/MAS ^{15}N NMR measurements also suggest that such rigidity of the mesogen groups may be due to the formation of intermolecular hydrogen bonding between NH and CO groups, and resulting segmental assemblies will induce the characteristic spacer conformation in the supercooled liquid crystalline component.

Introduction

During the past two decades, main-chain thermotropic liquid crystalline polymers have drawn both scientific and industrial attention on account of their excellent mechanical, optical, and thermal properties.[1−4] A number of research groups have reported syntheses and characterization for main-chain thermotropic liquid crystalline polymers with a variety of structural features and interconnecting units between the mesogenic groups and the flexible or rigid spacers, and those efforts have successfully led to the commercialization of thermotropic polyesters in addition to main-chain lyotropic aramides developed much earlier. Further developments of new engineering for such mesomorphic polymeric materials have been also greatly stimulated, including structural application, processing, blending, and self-reinforcing composite preparation. From a fundamental standpoint, recent research activity has concentrated on understanding of relationships between the chemical structure and properties and assessing specific aspects of the physical character for main-chain thermotropic liquid crystalline polymers. However, most of the attention has focused on a variety of thermotropic polyesters, and less frequent examples of other main-chain thermotropic liquid crystalline polymers consist of polyurethanes, polyethers, and so on.

Under such situations the first thermotropic liquid crystalline polyurethanes were synthesized from 3,3′-dimethyl-4,4′-biphenyldiyl diisocyanate and α,ω-alkanediols,[5] and a more systematic approach to the synthesis of tailor-made liquid crystalline polyurethanes was initiated by some research groups.[6−10] However, their developments were rather limited because of somewhat unstable and hazardous intermediates and monomers and more seriously owing to their low thermal stability at elevated temperatures. Nevertheless, systematic studies of the polyurethanes are very important for clarifying the role of the urethane moieties, particularly the role of hydrogen bonding, in affecting the structure and properties in the liquid crystalline state.[11] Through such fundamental investigations, it may be reasonable to presume that thermotropic liquid crystalline polyurethanes may find new applications ranging from surface coating to formulation of polymer blends or self-reinforcing composites with commercial polyamides and polyesters.

In a previous paper, we have characterized the crystalline−noncrystalline structure and chain conformation for a thermotropic main-chain liquid crystalline polyurethane (UDMB-10), which is built up from 3,3′-dimethyl-4,4′-biphenyldiyl diisocyanate, 1,10-decanediol, and 1-hexanol, in detail by high-resolution solid-state ^{13}C NMR spectroscopy.[12] In the sample crystallized by slowly cooling from the melt through the liquid crystalline state, it has been found that there exist three components with different spin−lattice relaxation times (T_{1C}), which are assigned to the crystalline, medium, and noncrystalline components, for the spacer CH_2 sequences. Moreover, the noncrystalline component, which corresponds to the supercooled liquid crystalline (LC) component, has been found to adopt the alternate *trans* and *trans*−*gauche* exchange conformation, prob-

10.1021/ma0202991 CCC: $22.00
Published on Web 06/06/2002

Scheme 1

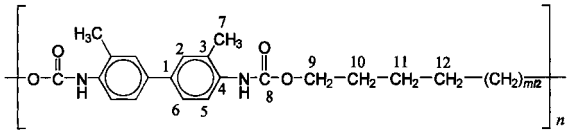

ably reflecting the conformation in the liquid crystalline state, whereas the crystalline and medium components are in the planar zigzag conformation.

In this paper, the effects of the spacer CH_2 length on the conformation are first examined for the main-chain liquid crystalline polyurethanes by using the similar solid-state ^{13}C NMR analysis employed previously.[12] To this end, liquid crystalline polyurethanes UDMB-*m* (*m* = 6, 8, 12), where *m* denotes the even number of spacer methylene carbons, are polymerized from 3,3′-dimethyl-4,4′-biphenyldiyl diisocyanate and α,ω-alkanediols having various even numbers *m* of carbons and 1-hexanol. Next, ^{13}C chemical shift anisotropy (CSA) analyses are carried out for the mesogen groups to clarify their molecular mobility. Natural abundant CP/MAS ^{15}N NMR measurements are also performed to discuss the role of hydrogen bonding on the characteristic spacer conformation and the molecular motion of the mesogen groups. Phase transition behavior and crystallizability of these polymers will be reported elsewhere together with the results for liquid crystalline polyethers with the same mesogen and spacer units but without hydrogen bonding.[13,14]

Experimental Section

Samples. 1,6-Hexanediol, 1,8-octanediol, 1,12-dodecanediol, and 1-hexanol were purchased from Nakalai Tesque in Kyoto, and 3,3′-dimethyl-4,4′-biphenyldiyl diisocyanate was provided from Nippon Soda Co., Ltd. These materials were used without further purification.

Polyurethanes UDMB-6, UDMB-8, and UDMB-12 were polymerized in anisole at 140 °C for 6 h with 3,3′-dimethyl-4,4′-biphenyldiyl diisocyanate as mesogen, 1,6-hexanediol, 1,8-octanediol, or 1,12-dodecanediol as spacer, and 1-hexanol as molecular weight controller in a molar ratio of 25/24/2.[5,12] The chemical structures of the polymers are shown in Scheme 1. The number-average molecular weights of the UDMB-6, UDMB-8, and UDMB-12 samples, which were determined by the end-group analyses using solution-state ^1H NMR spectroscopy, were 14 500, 17 900, and 18 700, respectively. Each sample for solid-state ^{13}C NMR measurements was crystallized under an argon atmosphere by cooling from the melt through the nematic phase at a rate of 1 °C/min for UDMB-6 and UDMB-8 or at a rate of 0.05 °C/min for UDMB-12.

Solid-State ^{13}C NMR Measurements. Solid-state ^{13}C NMR measurements were performed at room temperature on a JEOL JNM-GSX200 or Chemagnetics CMX200 spectrometer equipped with a JEOL variable temperature MAS system operating at 50.0 MHz under a static magnetic field of 4.7 T. ^1H and ^{13}C radio-frequency fields $\gamma B_1/2\pi$ were 62.5 kHz. The contact time for the CP process was 2.0 ms, and the recycle time after the acquisition of each free induction decay (FID) was 5 s throughout this work. The MAS rate was set to 3.6 kHz in order to avoid the overlapping of spinning sidebands on other resonance lines. ^{13}C chemical shifts were expressed as values relative to tetramethylsilane (Me_4Si) by using the CH_3 line at 17.36 ppm of hexamethylbenzene crystals as an external reference. ^{13}C spin−lattice relaxation times (T_{1C}) were measured by using the CPT1 pulse sequence.[15]

^{13}C CSA spectra were measured at room temperature by using the two-dimensional switching angle sample spinning (2D SASS) pulse sequence[16−19] shown in Figure 1, with the use of a Doty Scientific DAS probe. ^1H and ^{13}C radio-frequency field strengths $\gamma B_1/2\pi$ were 59.5 kHz, and the MAS rate was 7 kHz. The spinning angle θ_s was changed between 54.7° and 45° within about 10 ms in the pulse sequence. Solid-state natural abundant ^{15}N NMR measurements were carried out at room temperature on a Chemagnetics CMX-400 spectrometer under a static magnetic field of 9.4 T. ^1H and ^{15}N radio-frequency field strengths $\gamma B_1/2\pi$ were 41.7 kHz, and the MAS rate was 3 kHz.

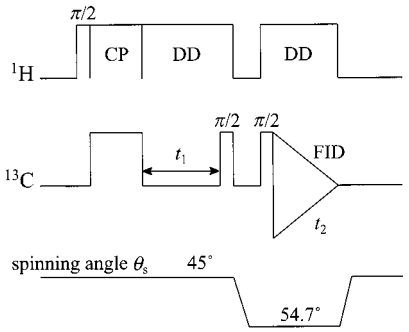

t_1 : incremented evolution time
t_2 : detection time

Figure 1. Pulse sequence for the two-dimensional switching angle sample spinning (2D SASS) method to measure ^{13}C chemical shift anisotropy.

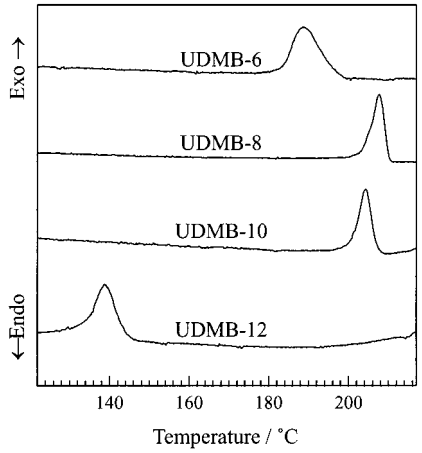

Figure 2. DSC thermograms of UDMB-*m* with *m* = 6−12 recorded on cooling at a rate of 1 °C/min.

Differential Scanning Calorimetry. A TA Instruments DSC2910 differential scanning calorimeter was used to measure the thermal transition behavior. The temperature was calibrated using indium. The differential scanning calorimetry (DSC) sample size ranged from 2.2 to 10.5 mg. All DSC runs were carried out under a nitrogen atmosphere at a rate of 10 °C/min. A first-order transition temperature was measured as a maximum or minimum of each transition peak.

Optical Microscopy. Thermal phase transition and texture changes were observed with a Nikon OPTIPHOT2-POL optical polarizing microscope equipped with a Linkam LK-600PM hot stage. Each powderlike sample was placed on a glass slide, covered with a glass coverslip, and heated or cooled under a nitrogen atmosphere in the hot stage at a rate of 10 °C/min.

Results and Discussion

Thermal Transition Behavior. DSC measurements and polarizing optical microscopic observations have been performed to confirm the existence of the liquid crystalline phase for the respective polyurethane samples. Figure 2 shows DSC thermograms measured for UDMB-6−UDMB-12 at a cooling rate of 1 °C/min. Only a single exothermic peak appears for these samples, in good accord with the case of UDMB-10 reported previously.[12]

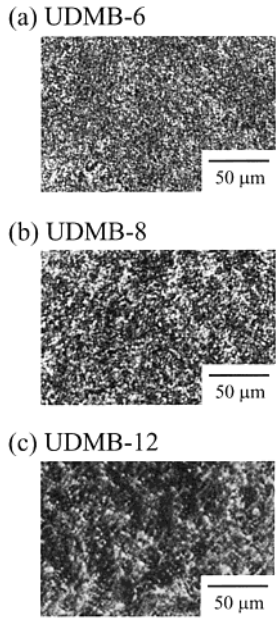

Figure 3. Polarizing optical microphotographs for UDMB-*m* with $m = 6-12$ on cooling at a rate of 1 °C/min, which were observed at about 197, 204, and 143 °C.

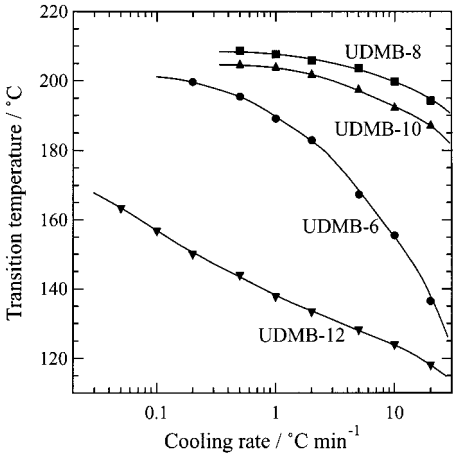

Figure 4. Plots of peak top temperatures of the exothermic peaks observed on the cooling process as a function of the cooling rate for UDMB-*m* with $m = 6-12$.

It should be, however, noted here that the exothermic peak of UDMB-12 is observed extraordinarily at a lower temperature compared to the peaks of the other samples. Figure 3 shows polarizing light micrographs for these samples taken at appropriate temperatures in the cooling processes at a rate of 1 °C/min. The texture seems rather unclear for UDMB-12 while UDMB-6 and UDMB-8 show the nematic phase texture. Moreover, two clear peaks corresponding to the crystalline−nematic and nematic−isotropic phase transitions were not observed for UDMB-12 on the second heating run, whereas such two peaks clearly appeared like the case of UDMB-10.[12] Since this fact may be due to the slower rate of the phase transition for UDMB-12 on cooling, we have performed DSC measurements at various cooling rates and examined the cooling rate dependencies for all samples including UDMB-10.

In Figure 4 peak top temperatures of the exothermic peaks observed on the cooling process are plotted against the cooling rate for each sample. As is clearly seen in this figure, there are large differences in cooling rate dependence among these samples: UDMB-8 and UDMB-10 have the smaller dependencies, and their transition temperatures seem to become constant at cooling rates slower than about 1 °C/min. In contrast, UDMB-6 and UDMB-12 show larger cooling rate dependencies, particularly no level-off tendency being observed for UDMB-10 even around 0.05 °C/min. Considering these results, UDMB-6, UDMB-8, and UDMB-10 were cooled at 1 °C/min from the melt at 220 °C whereas UDMB-12 was done at 0.05 °C/min. The latter rate may be the slow limit for DSC measurements without significant degradation at higher temperatures for the polyurethane samples.

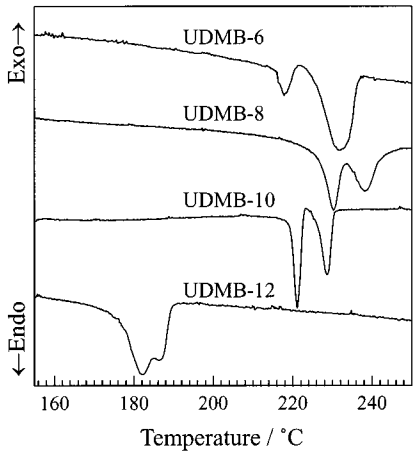

Figure 5. DSC thermograms for UDMB-*m* with $m = 6-12$ recorded on the second heating at a rate of 1 °C/min.

Figure 5 shows DSC heating thermograms obtained for these samples at a heating rate of 1 °C/min. Two endothermic peaks are found to clearly appear for the respective samples including UDMB-12. Furthermore, polarizing optical microscopy observations have confirmed that the nematic phase forms in the temperature region between the two DSC peaks for each sample shown in Figure 5. Therefore, the two endothermic peaks are ascribed to the crystalline−nematic and nematic−isotropic phase transitions in the order of increasing temperature. On the basis of these DSC results, the UDMB-6, UDMB-8, and UDMB-12 samples for solid-state NMR measurements were prepared by cooling from the melt at rates of 1, 1, and 0.05 °C/min, respectively.

CP/MAS ^{13}C NMR Spectra. The 50 MHz CP/MAS ^{13}C NMR spectra of the UDMB-6, UDMB-8, and UDMB-12 samples measured at room temperature are shown in Figure 6. For comparison, the solution-state ^{13}C NMR spectrum of UDMB-8 measured at 100 °C in deuterated dimethyl sulfoxide (DMSO-d_6) is also shown in this figure. The assignment of the respective resonance lines for each sample has been made on the basis of the solution-state spectra for the corresponding samples and the assignment previously made for UDMB-10.[12]

^{13}C Spin−Lattice Relaxation Behavior. To examine the crystalline−noncrystalline structure for each polyurethane sample, ^{13}C spin−lattice relaxation behavior has been measured at room temperature by the CPT1 pulse sequence.[15] The analyses of the decay curves have been performed in terms of two or three components having different T_{1C} values by the computer-aided nonlinear least-squares method in the same way as performed for the case of UDMB-10.[12] In Table 1 the T_{1C} values of the respective carbons are summarized for all samples obtained at room temperature. For com-

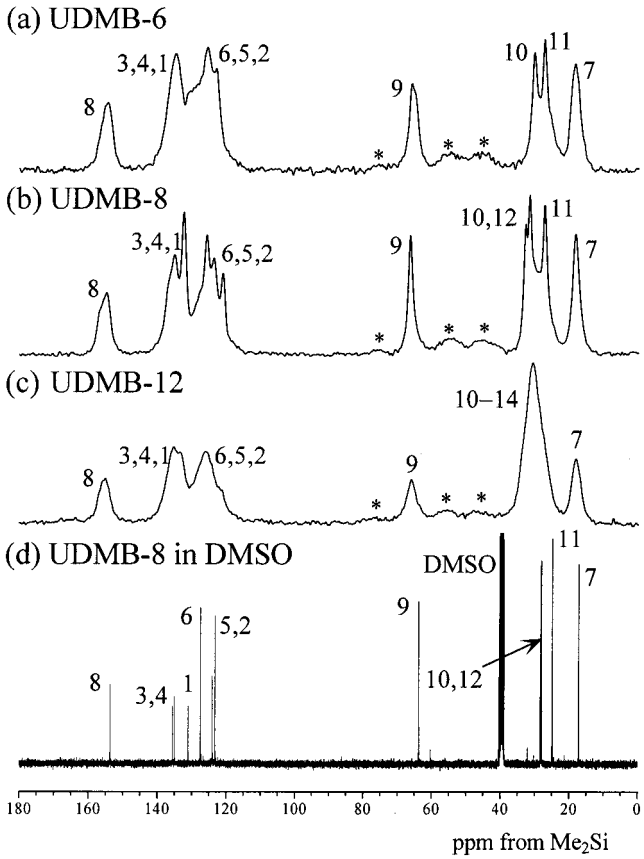

Figure 6. ^{13}C NMR spectra for UDMB-*m*: (a−c) 50 MHz CP/MAS ^{13}C NMR spectra measured for UDMB-*m* with $m = 6$, 8, and 10 at room temperature; (d) 100 MHz solution-state ^{13}C NMR spectrum measured for UDMB-8 at 100 °C. * indicates a spinning sideband.

parison, the corresponding T_{1C} values for UDMB-10 reported previously[12] are also filed in this table. For any of four samples, the spacer CH_2 carbons are found to contain three components with different T_{1C} values that are assigned to the crystalline, medium, and noncrystalline components according to the previous assigment.[12] In contrast, only two T_{1C} values were detected for the mesogen carbons including the methyl and carbonyl carbons for each sample as shown in Table 1. Since the mesogen groups have bulky and rigid structure, molecular mobility may be not highly enhanced even in the noncrystalline region when the CH_2 sequences in this region are allowed to have much higher molecular mobility as detected as the component with T_{1C} values shorter than 1 s. Such low molecular mobility of the mesogen groups may lead to the detection of two T_{1C} values as a result of simple discrimination between more and less mobile components in this system. Somewhat more detailed discussion will be made later after measuring ^{13}C CSA spectra of the mesogen carbons.

Conformations of the Methylene Sequences. (a) UDMB-8. Figure 7 shows ^{13}C NMR spectra of the crystalline, medium, and noncrystalline components for the methylene carbons in UDMB-8, which have been separately recorded by using the difference in T_{1C} for the three components as follows: The spectrum of the crystalline component has been selectively measured by the CPT1 pulse sequence[15] by setting the T_{1C} decay time τ to 80 s. On the other hand, the spectrum of the medium component has been obtained by subtracting the spectrum of the crystalline component from the spectrum measured by the CPT1 pulse sequence with $\tau = 5$ s, which is long enough to completely suppress only the noncrystalline contribution. As for the noncrystalline component, the spectrum has been measured by the saturation recovery pulse sequence modified for solid-state measurements[20,21] by setting the T_{1C} recovery time to 1 s, although some minor contribution from other components is included in this spectrum.

The chemical shifts of the C9−C12 resonance lines for the crystalline component are in good accord with those for the medium component. This fact suggests that both components have the same chain conformation for the spacer CH_2 sequences, probably the planar zigzag conformation like the case of UDMB-10.[12] In contrast, the C10 and C12 resonance lines for the noncrystalline component significantly shift upfield compared to the corresponding lines for the crystalline and medium components, while the chemical shifts of the C9 and C11 lines stay unaltered. To examine the conformation of the methylene sequences for each component by considering the *γ-gauche* effect,[22] line shape analyses have been carried out for the crystalline and noncrystalline components.

Figure 8a shows the result of the line shape analysis for the spectrum of the crystalline component. Here, each line is assumed to be described by a Lorentzian curve. It is clearly found that the resonance lines located at about 35−30 ppm are well resolved into two Lorentzian curves, which correspond to the resonance lines for the C10 and C12 carbons. Moreover, the respective resonance lines appearing at about 27 and 18 ppm are well fitted by single Lorentzians which correspond respectively to the C11 and C7 carbons. Their chemical shifts are also in good accord with the corresponding values of the crystalline component for UDMB-10.[12] It is, therefore, assumed as made for UDMB-10[12] that the methylene sequence of the crystalline component for UDMB-8 is in the *all-trans* conformation. This assumption is highly reasonable because there are previous reports for main-chain liquid crystalline polymers[23,24] that support this assumption.

In Figure 8b is shown the result of the line shape analysis for the spectrum of the noncrystalline component. This spectrum also contains a small amount of the contributions from the medium component, since the T_{1C} values of the medium component are not sufficiently long compared to those for the noncrystalline component. Therefore, the line shape analysis has been performed considering such contributions from the medium component in addition to the three Lorentzian curves for the C10, C11, and C12 carbons for the noncrystalline component. In this case the chemical shifts values of the two Lorentzian curves obtained through the line shape analysis for the spectrum of the crystalline component are used for the two Lorentzians of the medium component because their chemical shifts should agree with each other as seen in Figure 7. The thick broken line, which is a composite curve of the six Lorentzians denoted by thin broken lines, is in good accordance with the experimental spectrum indicated by a solid line.

It should be first noted that the chemical shifts for the C9 and C11 carbons of the noncrystalline component are in good accord with their values for the crystalline component as described above. Since the chemical shifts of the C9 and 11 carbons are respectively determined

Table 1. ^{13}C Spin−Lattice Relaxation Times of UDMB-*m* with *m* = 6−12 Measured at Room Temperature

	T_{1C}/s						
	spacer				mesogen		
component	CH_2[a]	CH_2[b]	OCH_2	C=O	q-C[c]	CH[d]	CH_3
UDMB-6							
crystalline	84.2	82.3	77.5	165	113	95.2	38.3
medium	6.4	9.4	5.4	22.2	14.1	12.4	5.9
noncrystalline	0.42	0.49	0.49				
UDMB-8							
crystalline	265	246	238	189	245	251	68.8
medium	14.6	24.9	9.5	14.8	24.0	21.3	7.7
noncrystalline	0.42	0.65	0.42				
UDMB-10[e]							
crystalline	227	191	191	165	212	187	65.3
medium	22.6	13.3	18.8	22.2	19.0	10.8	6.5
noncrystalline	1.0	0.48	0.95				
UDMB-12							
crystalline	116	102	115	165	94.5	112	55.4
medium	3.7	3.0	3.4	22.2	16.1	8.0	5.8
noncrystalline	0.33	0.22	0.22				

[a] At 32 ppm. [b] At 27 ppm. [c] Quaternary carbons; at 133 ppm. [d] At 125 ppm. [e] Reference 12.

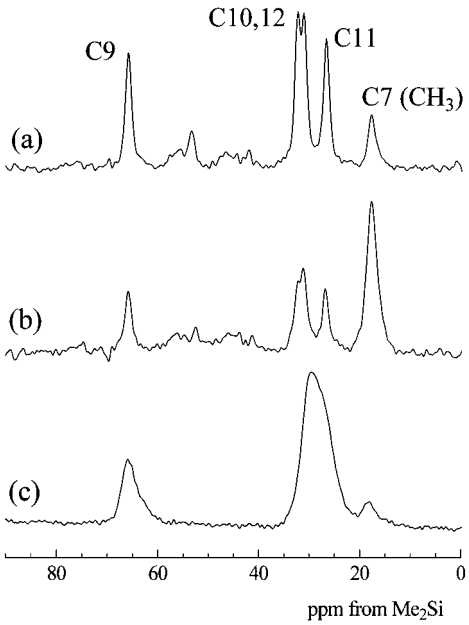

Figure 7. ^{13}C NMR spectra of different components separately recorded at room temperature for UDMB-8 which was crystallized from the melt through the liquid crystalline phase by cooling at a rate of 1 °C/min: (a) crystalline, (b) medium, and (c) noncrystalline.

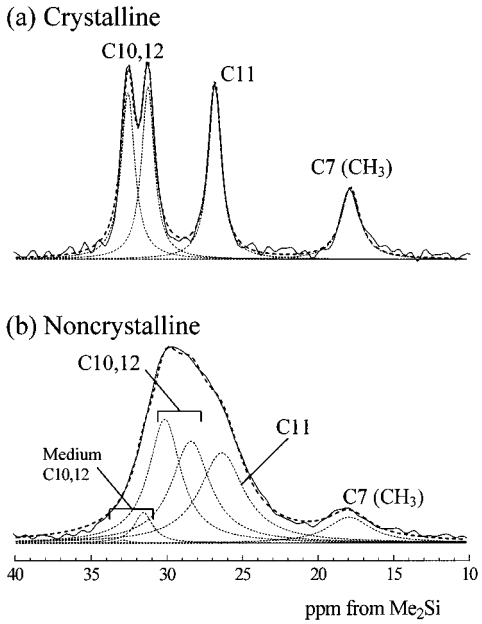

Figure 8. Line shape analysis for the CH_2 resonance lines for the UDMB-8 sample shown in Figure 7: (a) crystalline; (b) noncrystalline.

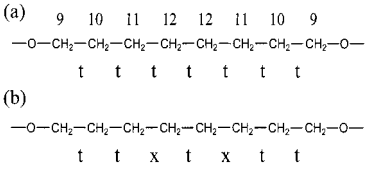

Figure 9. Chain conformations for the spacer CH_2 sequences in different components in the UDMB-8 sample shown in Figure 7: (a) crystalline and medium; (b) noncrystalline. *t* and *x* indicate *trans* and *trans*−*gauche* exchange conformations, respectively.

by the conformations of the C10−11 bond and C9−C10/C12−C12 bonds, the C9−C10, C10−C11, and C12−C12 bonds of the noncrystalline component should also adopt the *trans* conformation like the case of the crystalline component. In contrast, if the extent of the *γ-gauche* effect[22] is assumed to be almost the same for the C10 and C12 carbons, these resonance lines may undergo about 2.5 ppm upfield shifts compared to the values for the crystalline component. The validity of this assumption is discussed below. Then, this fact indicates that these CH_2 carbons are subjected to about a half of the *γ-gauche* effect probably originating from one second-neighboring C−C bond having the rapid *trans*−*gauche* exchange conformation. It is, therefore, concluded that the C11−C12 bonds are in the *trans*−*gauch*e exchange conformation (*x*) while the other bonds adopt the *trans* conformation, as shown in Figure 9.

It should be noted here that the extent of the *γ-gauche* effect may be different for the C10 and C12 carbons, because the assignment of these carbon resonance lines have not yet been established for both crystalline and noncrystalline components. In that case the C10 and C12 lines for the noncrystalline component will undergo about 1.0 and 4.0 ppm upfield shifts (a) or vice versa (b) compared to those of the crystalline component, respectively. In the former case (a), the evaluation of the chemical shifts by considering the *γ-gauche* effect suggests that the C11−C12 bonds in the noncrystalline

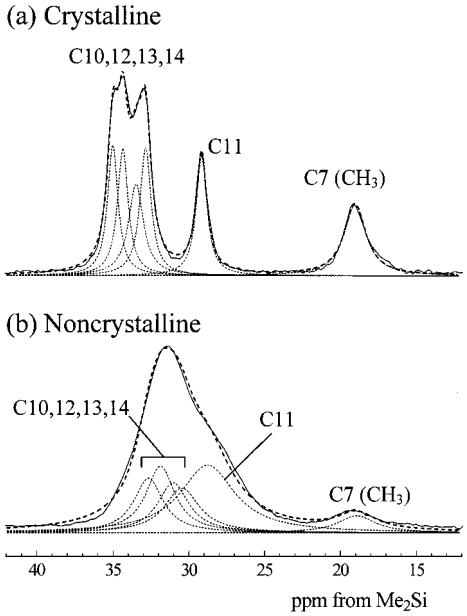

Figure 10. Line shape analysis for the CH_2 resonance lines for the UDMB-12 sample which was crystallized from the melt through the liquid crystalline phase by cooling at a rate of 0.05 °C/min: (a) crystalline; (b) noncrystalline.

component may adopt the *trans*−*gauche* exchange conformation with a *trans*/*gauche* probability ratio of 2/8, and the *gauche* conformation should be introduced to the O−C9 bonds in both crystalline and noncrystalline components. Such conformations may be unrealistic in the noncrystalline state which corresponds to the supercooled liquid crystalline state, and the *gauche* introduction must be energetically rejected in the crystalline region for the polyurethane sample. The latter case (b) also suggests similar unrealistic conformations for the present sample. It should be, therefore, plausible to assume that the C10 and C12 carbons are subjected to the same extent of the *γ-gauche* effect, as made above.

(b) UDMB-12. Figure 10 shows solid-state ^{13}C NMR spectra of the crystalline and noncrystalline components for the CH_2 carbons in UDMB-12, which were separately recorded by using the difference in T_{1C} in a fashion similar to the case of UDMB-8. The chemical shifts of the respective C9−C14 resonance lines for the crystalline and medium components are also in good accord with each other, indicating that both components adopt the same chain conformation. In contrast, the C10, C12, C13, and C14 resonance lines for the noncrystalline component significantly shift upfield compared to the corresponding lines for the crystalline and medium components, while the chemical shifts of the C9 and C11 lines stay constant for all the components. To examine the conformation of the methylene sequence for each component in detail by analyzing the chemical shifts of the respective lines considering the *γ-gauche* effect,[22] line shape analyses have been also carried out for the crystalline and noncrystalline components.

Figure 10a also shows the result of the line shape analysis for the spectrum of the crystalline component. The chemical shifts of the respective Lorentzian curves well resolved are in good accord with those of the crystalline component for UDMB-10[12] and UDMB-8, indicating that the methylene sequence of the crystalline component for UDMB-12 will be also in the *all-trans* conformation. In Figure 10b is shown the result of the line shape analysis for the spectrum of the noncrystalline component. As is clearly seen in this figure, the composite curve indicated as a thick broken line, which is composed of six Lorentzians denoted by thin broken lines, is in good accordance with the experimental spectrum indicated by a thick solid line. Since the chemical shifts for the C9 and C11 carbons well agree with the corresponding values obtained for the crystalline component in Figure 10a, the C9−C10, C10−C11, C12−C13, and C14−C14 bonds should adopt the trans conformation. In contrast, for the C10, C12, C13, and C14 carbons, the chemical shifts of the four corresponding Lorentzians seem to undergo about 2.5 ppm upfield shifts from the values for the crystalline component under the same assumption that the extent of the *γ-gauche* effect is almost the same for each carbon as made above for the case of UDMB-8. Accordingly, these respective carbons have the *γ-gauche* effect associated with one C−C bond adopting the rapid *trans*−*gauche* exchange conformation in the same fashion as the cases of UDMB-8 and UDMB-10. As a result, such a *γ-gauche* effect for the C10, C12, C13, and C14 resonance lines should be induced from the C11−C12 and C13−C14 bonds. It is, therefore, concluded that the C11−C12 and C13−C14 bonds are in the *trans*−*gauche* exchange conformation (*x*) as illustrated in Figure 11.

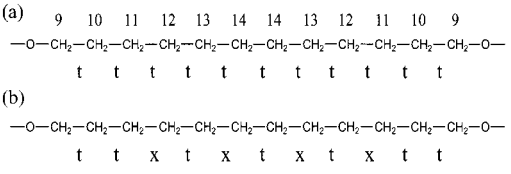

Figure 11. Chain conformations for the spacer CH_2 sequences in different components in the UDMB-12 sample shown in Figure 10: (a) crystalline and medium; (b) noncrystalline. *t* and *x* indicate *trans* and *trans*−*gauche* exchange conformations, respectively.

General Description. On the basis of the results of UDMB-8 and UDMB-12 obtained in this work as well as the results of UDMB-10 described in the previous paper,[12] the conformations of the spacer CH_2 sequences for the noncrystalline component will be generally expressed as $ttx(tx)_l tt$ ($l = m/2 - 3$) for $8 \leq m \leq 12$. Unfortunately, a similar analysis could not be applied to the case of UDBM-6, because the spacer CH_2 sequences seem not to adopt the simple planar zigzag conformation in the crystalline region for this sample. Further detailed analyses will be necessary for UDMB-6.

In contrast to the polyurethane samples, a newly synthesized liquid crystalline polyether (EDBM-10), which is composed of the same mesogen and spacer units as for UDBM-10, provides an interesting result; a similar alternate *t* and *x* conformation *txtxtxtxt* was found to be allowed for the CH_2 sequences *in the crystalline region*.[14] Moreover, separate molecular dynamics simulations in the crystalline state for the polyether EDMB-10 revealed that a pair of *gauche*$^+$ and *gauche*$^-$ are introduced in the corresponding alternate C−C bonds in each CH_2 sequence, and their *trans*/*gauche* probabilities are about 0.5, in good accord with the experimental result, while all the other C−C bonds always adopt the *trans* conformation.[25] This fact implies that such a characteristic alternate *t* and *x* conformation may be definitely induced to keep the molecular chain axis almost constant in the crystalline state when the

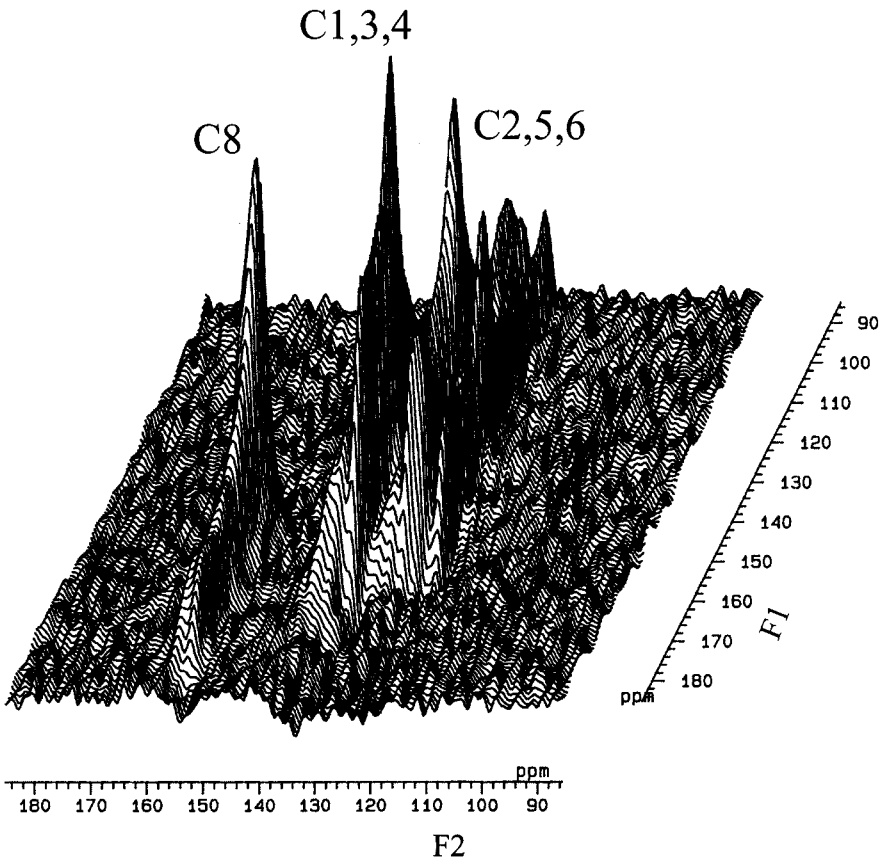

Figure 12. 2D SASS ^{13}C NMR spectrum measured at room temperature for the carbonyl and phenylene carbons of the UDMB-10 sample.

spacer CH_2 sequences undergo much enhanced molecular motion.

However, similar simulations were not effectively performed to examine the liquid crystalline state for the polyurethane UDMB-10 probably because it was still difficult to set an appropriate polymer consistent force field[26] for the realization of the liquid crystalline state of this polymer. Nevertheless, it seems plausible to point out that the alternate *t* and *x* conformation may be also allowed to keep the orientation of the spacer groups almost constant even in the supercooled liquid crystalline state for the polyurethanes. Moreover, some aggregation structure of the mesogen groups possibly through hydrogen bonding should be closely associated with the production of the alternate *t* and *x* conformation, because the spacer CH_2 sequences were found to adopt the random conformation described as *xxxxxxxxx* in the supercooled liquid crystalline component for EDMB-10 with no hydrogen bonding.[14] To examine molecular mobility and hydrogen bonding for the mesogen groups in the polyurethane samples, natural abundant ^{15}N NMR measurements have been conducted as described below.

Molecular Motion and Hydrogen Bonding of the Mesogen Units. As seen in Table 1, the T_{1C} values of the mesogen aromatic carbons are about 180−210 s for the less mobile component which may be composed of the whole crystalline component and a part of the medium component. This fact indicates that the mesogen units in this component are highly inhibited in molecular mobility on a time scale of 10^{-8} s associated with the T_{1C} relaxation. In contrast, the T_{1C} values are much reduced to about 11−19 s for the mobile component that may contain a residual part of the medium component and the noncrystalline component. This fact suggests that the phenylene rings may undergo the so-called 180° flip motion or the random fluctuation with relatively large amplitudes around the phenylene axis in this component.

To examine molecular motion of the mesogen units in detail, ^{13}C CSA spectra have been measured for the mesogen carbons by 2D SASS ^{13}C NMR spectroscopy.[16−19] Figure 12 shows the 2D SASS ^{13}C NMR spectrum in the aromatic carbon region, measured at room temperature for UDMB-10 which was crystallized from the melt by cooling at a rate of 1 °C/min. Since overlapping of the respective CSA contributions is still serious in this figure, an overhead view along the F1 axis for the C2, 5, and 6 carbons is shown in Figure 13a. The CSA line shape is clearly observed for each isotropic contribution along the F2 axis, although the assignment has not been established for these carbons as indicated in Figure 6. Here, the remarkable reduction in intensity appearing in the central part between σ_{11} and σ_{22} or between σ_{22} and σ_{33} will be due to slow sample spinning.[27]

The computer-simulated CSA spectra, which were obtained by using the two-site exchange model for the flip motions of the phenylene group with different flip angles,[18,19] are shown in Figure 13b. Here, the principal values of the chemical shift tensor for the ortho CH carbons of the analogous systems were used: $\sigma_{11} = 216$ ppm, $\sigma_{22} = 135$ ppm, and $\sigma_{33} = 7$ ppm.[28] Moreover, the flip rate is assumed to attain to the fast limit ($>\sim 10^5$ s^{-1}). The line shapes of the simulated spectra with the flip angles less than 20° seem to be in good accord with the experimental spectra shown in Figure 13a. This result suggests that the flip angles of fluctuations

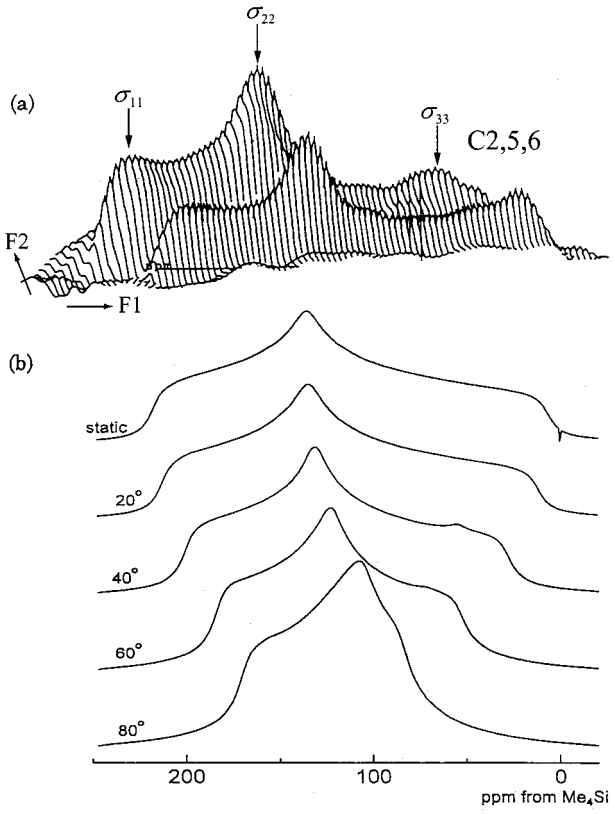

Figure 13. ^{13}C CSA spectra for the phenylene ortho carbons: (a) experimental; (b) simulated spectra for different flip angles under the fast limit condition.

around the C1−C4 phenylene axis may be limited to less than about 20° in all components existing in UDMB-10, including the noncrystalline (supercooled liquid crystalline) component. The 180° flip motion is found not to occur in this sample because the CSA spectrum for the aromatic CH carbons undergoing that flip motion markedly differs from the rigid CSA spectrum as a result of the average of the σ_{11} and σ_{22} components.[18] It should be also noted that there is no difference in slower molecular motion with rates of about 10^5 s^{-1} associated with CSA in the three or two components which are detected by T_{1C} values associated with faster molecular motion with rates of about 10^8 s^{-1}. In addition, almost the same CSA spectra were obtained for UDMB-8 and UDMB-12, indicating similar restriction in molecular mobility for the mesogen groups in these samples.

Since such restricted molecular mobility for the mesogen groups may be due to intermolecular hydrogen bonding between the NH and CO units, a natural abundant CP/MAS ^{15}N NMR spectrum have been measured at room temperature for UDMB-8 as shown in Figure 14. A single resonance line can be clearly observed at about 55 ppm, which is expressed as a chemical shift value relative to the ^{15}N resonance line for NH_4Cl powdered crystals as an external reference. Moreover, a ^{15}N T_1 measurement performed by the CPT1 pulse sequence[15] has revealed that the single resonance line at about 55 ppm contains two components with $T_{1N} = 470$ and 15 s, which correspond to the two components with different T_{1C} values as shown in Table 1. It is, therefore, concluded that the crystalline and supercooled liquid crystalline components have the same ^{15}N chemical shift values in the polyurethane samples. Since a recent report[29] shows that ^{15}N chemical

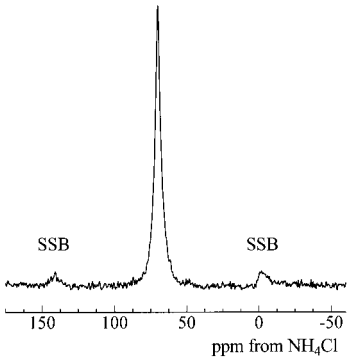

Figure 14. Natural abundant CP/MAS ^{15}N NMR spectrum measured at room temperature for the UDBM-8 sample.

shifts strongly depend on the N−H length in the NH···CO hydrogen bonding for oligopeptides, the supercooled liquid crystalline component must be in almost the same intermolecular hydrogen bonding state as for the crystalline component. Such hydrogen bonding among the mesogen units will produce some kinds of segmental assemblies even in the supercooled liquid crystalline region, resulting in less molecular mobility of the mesogen units as revealed by the CSA analysis. Moreover, the characteristic spacer conformation described above may be allowable in such a segmental assembly state for the polyurethane samples. Further discussion will be made after the characterization of the phase transition behavior and dynamics of a liquid crystalline polyether EDMB-10 with the same mesogen and spacer units as for UDMB-10 and, therefore, without hydrogen bonding.

Conclusions

The structure and dynamics of the spacer CH_2 sequences and the mesogen groups for liquid crystalline polyurethanes with different spacer lengths have been characterized for the samples crystallized by slowly cooling from the melt through the liquid crystalline state by solid-state ^{13}C and ^{15}N NMR analyses, and the following conclusions have been obtained:

(1) ^{13}C spin−lattice relaxation time (T_{1C}) analyses have revealed that there exist three components with different T_{1C} values for the spacer CH_2 sequences in each sample at room temperature. These components are assigned to the crystalline, medium, and noncrystalline (or supercooled liquid crystalline) components in the order of decreasing T_{1C} values.

(2) The spectra of the respective components involved in the UDMB-8 and UDMB-12 samples have been separately recorded by using the difference in T_{1C}, and the line shape analysis in the CH_2 carbon region of each spectrum has been successfully performed to resolve the spectrum to the respective CH_2 carbon contributions.

(3) The conformation of the CH_2 sequences in each component for UDMB-8 and UDMB-12 has been clarified by the evaluation of ^{13}C chemical shifts obtained by the line shape analyses described above in terms of the *γ-gauche* effect. In the crystalline and medium components, the CH_2 sequences are suggested to be in the planar zigzag conformation, in good accord with the case of UDMB-10. In contrast, the CH_2 sequences of the noncrystalline component are found to adopt the alternate *trans* (*t*) and *trans*−*gauche* exchange (*x*) conformations: *ttxtxtt* for UDMB-8 and *ttxtxtxtxtt* for UDMB-12. Considering also the result for UDMB-10 previously

reported, the spacer CH_2 conformation of the noncrystalline component is generally expressed as $ttx(tx)_{\ell}tt$ ($\ell = m/2 - 3$) for $8 \leq m \leq 12$ for the polyurethanes.

(4) The ^{13}C chemical shift anisotropy analysis has revealed that the mesogen units are highly hindered in molecular mobility even in the supercooled LC component. Natural abundant CP/MAS ^{15}N NMR measurements suggest that such less mobility of mesogen units may be due to the formation of some kinds of segmental assemblies through intermolecular hydrogen bonding between NH and CO groups, and the characteristic spacer conformation described above will be also induced in such a segmental assembly state.

Acknowledgment. This work was supported by Grant-in-Aid for Scientific Research (No. 12450384) from the Ministry of Education, Culture, Sports, Science and Technology, Japan.

References and Notes

(1) Isayev, A. I., Kyu, T., Cheng, S. Z. D., Eds.; *Liquid-Crystalline Polymer Systems. Technological Advances*; ACS Symposium Series 632; American Chemical Society: Washington, DC, 1996.
(2) Collings, P. J., Patel, J. S., Eds.; *Handbook of Liquid Crystal Research*; Oxford University Press: New York, 1997.
(3) Ward, I. M., Ed.; *Structure and Properties of Oriented Polymers*; Chapman & Hall: London, 1997.
(4) Chung, T.-S., Ed.; *Thermotropic Liquid Crystal Polymers*; Technomic: Lancaster, 2001.
(5) Iimura, K.; Koide, N.; Tanabe, H.; Takeda, M. *Macromol. Chem.* **1981**, *182*, 2569.
(6) Tanaka, M.; Nakaya, T. *Macromol. Chem.* **1989**, *190*, 3067.
(7) Smyth, G.; Vallés, E. M.; Pollack, S. K.; Grebowicz, J.; Stenhouse, P. J.; Hsu, S. L.; McKnight, W. J. *Macromolecules* **1990**, *23*, 3389.
(8) Mormann, W.; Brahm, M. *Macromolecules* **1991**, *24*, 1096.
(9) Kricheldorf, H. R.; Awe, J. *Macromol. Chem.* **1989**, *190*, 2579, 2597.
(10) Chiellni, E.; Galli, G.; Trusendi, S.; Angeloni, S. A.; Laus, M.; Francescangeli, O. *Mol. Cryst. Liq. Cryst.* **1994**, *243*, 135.
(11) Pollack, S. K.; Smyth, G.; Papadimitrakopoulos, F.; Stenhouse, P. J.; Hsu, S. L.; McKnight, W. J. *Macromolecules* **1992**, *25*, 2381.
(12) Ishida, H.; Kaji, H.; Horii, F. *Macromolecules* **1997**, *30*, 5799.
(13) Murakami, M.; Miyazaki, M.; Ishida, H.; Horii, F. *Polym. Prep. Jpn.* **2000**, *49*, 2359.
(14) Ishida, H.; Horii, F. *Macromolecules* **2001**, *34*, 7751.
(15) Torchia, D. A. *J. Magn. Reson.* **1981**, *44*, 117.
(16) Bax, A.; Szeverenyi, N. M.; Maciel, G. E. *J. Magn. Reson.* **1983**, *55*, 494.
(17) Terao, T.; Fujii, T.; Onodera, T.; Saika, A. *Chem. Phys. Lett.* **1984**, *107*, 145.
(18) Horii, F.; Beppu, T.; Takaesu, N.; Ishida, M. *Magn. Reson. Chem.* **1994**, *32*, 30.
(19) Horii, F. In *NMR Relaxations and Dynamics, in Solid State NMR of Polymers*; Ando, I., Asakura, T., Eds.; Studies in Physical and Theoretical Chemistry Vol. 84; Elsevier Sci.: Amsterdam, 1998.
(20) Kitamaru, R.; Horii, F.; Murayama, K. *Macromolecules* **1986**, *19*, 639.
(21) Hirai, A.; Horii, F.; Kitamaru, R.; Fatou, J. G.; Bello, A. *Macromolecules* **1990**, *23*, 2913.
(22) Tonelli, A. E. *NMR Spectroscopy and Polymer Microstructure: The Conformational Connection*; VCH Publishers: New York, 1989.
(23) Cheng, J.; Jin, Y.; Wunderlich, B.; Cheng, S. Z. D.; Yandrasits, M. A.; Zhang, A.; Percec, V. *Macromolecules* **1992**, *25*, 5991.
(24) Cheng, J.; Jin, Y.; Chen, W.; Wunderlich, B.; Jonsson, H.; Hult, A.; Gedde, U. W. *J. Polym. Sci., Part B: Polym. Phys.* **1994**, *32*, 721.
(25) Ishida, H.; Maekawa, Y.; Horii, F.; Yamamoto, T. *Polym. Prepr., Jpn* **2001**, *50*, 2342.
(26) Maple, J. R.; Hwang, M.-J.; Stockfisch, T. P.; Dinur, U.; Waldman, M.; Ewig, C. S.; Hagler, A. T. *J. Comput. Chem.* **1994**, *15*, 162.
(27) Hwang, M.-J.; Stockfisch, T. P.; Hagler, A. T. *J. Am. Chem. Soc.* **1994**, *116*, 2515.
(28) Sun, H.; Mumby, S. J.; Maple, J. R.; Hagler, A. T. *J. Am. Chem. Soc.* **1994**, *116*, 2978.
(29) Sethi, N. K.; Alderman, D. W.; Grant, D. M. *Mol. Phys.* **1990**, *71*, 217.
(30) Duncan, T. M. *A Compilation of Chemical Shift Anisotropies*: Farragut Press: Chicago, 1990.
(31) Ando, I.; Kameda, T.; Asakawa, N. In *Polypeptides, in Solid State NMR of Polymers*; Ando, I., Asakura, T., Eds.; Studies in Physical and Theoretical Chemistry Vol. 84; Elsevier Sci.: Amsterdam, 1998.

MA0202991